

THERMO-ECONOMIC ANALYSIS OF DUAL-PRESSURE EVAPORATION ORGANIC RANKINE CYCLE SYSTEM USING R245FA

Jian Li¹, Yuanyuan Duan^{1*}, Zhen Yang¹

¹Key Laboratory for Thermal Science and Power Engineering of MOE, Tsinghua University, Beijing, PR China
yyduan@tsinghua.edu.cn

* Corresponding Author

ABSTRACT

Dual-pressure evaporation cycle is an emerging cycle type in the organic Rankine cycle (ORC) field, which remarkably increases the conversion efficiency, and the adaptability to various heat sources is better compared with the conventional single-pressure evaporation cycle. However, the published studies on the dual-pressure evaporation cycle are mainly limited to the thermodynamic performance. The studies on the thermo-economic performance are insufficient to date. This study analyzed the thermo-economic performance of dual-pressure evaporation ORC system using R245fa for heat sources of 100–200°C. The heat exchangers are shell-and-tube type and the working fluid flows in the tubes. The effects of heat source temperature, mass flow rate of heat source fluid, and pinch point temperature differences (PPTDs) on the system thermo-economic performance were quantitatively analyzed. The thermo-economic performance of single-pressure and dual-pressure evaporation cycles was compared. Results show that the specific investment cost (*SIC*) of dual-pressure evaporation ORC system decreases as the heat source temperature increases. Increasing the mass flow rate of heat source fluid will substantially reduce the *SIC*. Increasing the PPTDs is beneficial to reduce the *SIC* at a high heat source temperature. The purchased costs of heat absorbers and condenser are two largest terms in the system, and their ratios to the total purchased equipment cost are 30.9%–49.5% and 32.9%–43.7%, respectively. The *SIC* of dual-pressure evaporation cycle increases by 5.7%–14.2% compared to the single-pressure evaporation cycle, and that is mainly ascribed to the remarkable increase in the purchased cost of heat absorbers.

1. INTRODUCTION

Organic Rankine cycle (ORC) is a promising heat-power conversion system for the widespread use of medium to low grade thermal energy since it is efficient, stable, flexible, safe and applicable to wide range of installed capacity (Imran *et al.*, 2018; Velez *et al.*, 2012; and Ziviani *et al.*, 2014). Selection and improvement of cycle structure are always hot study issues in the ORC field because the cycle structure significantly affects the system performance (Lecompte *et al.*, 2015; and Li *et al.*, 2017b).

The dual-pressure evaporation cycle is emerging in the ORC field (Lecompte *et al.*, 2015), which has two evaporation processes with different pressures and a condensation process (Li *et al.*, 2018). Compared to the conventional subcritical cycle with a single evaporation pressure, the dual-pressure evaporation cycle can substantially reduce the exergy loss between heat source and working fluids and thereby increase the conversion efficiency of ORC system (Li *et al.*, 2018; and Sadeghi *et al.*, 2016). Furthermore, the adaptability of dual-pressure evaporation cycle to various heat sources is also better since it has more cycle parameters can be actively optimized in the heat absorption process (i.e., the heat transfer process between heat source and working fluids) (Li *et al.*, 2019). The great superiority of dual-pressure evaporation cycle in the thermodynamic performance has been confirmed by several studies. For example, Li *et al.* (2018) found that the power output of dual-pressure evaporation cycle increased by 21.4%–26.7% than that of single-pressure evaporation cycle for nine

pure fluids. The results of Li *et al.* (2019) indicated that the maximum power output of dual-pressure evaporation cycle could increase by 25.7% at most compared with that of single-pressure evaporation cycle for isobutane/isopentane mixtures. Shokati *et al.* (2015) showed that the power output of dual-pressure evaporation cycle increased by 15.2%, 35.1%, and 43.5% compared with the single-pressure evaporation, cascade, and Kalina cycles, respectively. Furthermore, the studies on the dual-pressure evaporation ORC system are increasing.

The thermodynamic performance superiority of dual-pressure evaporation cycle is based on the reduction of heat transfer temperature difference between heat source and working fluids. The exergy loss is substantially reduced. However, the purchased cost of heat absorbers will be remarkably increased due to the increase of heat transfer area, which will increase the system investment cost and may even weaken the thermo-economic performance. However, the published studies on the dual-pressure evaporation ORC system are mainly limited to the thermodynamic performance. The studies on the thermo-economic performance are insufficient to date. To evaluate the application potential of dual-pressure evaporation cycle more comprehensively, a systematical comparison of thermo-economic performance between single-pressure and dual-pressure evaporation cycles needs to be carried out. Moreover, the heat source temperature, mass flow rate of heat source fluid, and pinch point temperature differences (PPTDs) in the cycle heat transfer processes significantly affect the thermo-economic performance of ORC system. The effects of these factors on the thermo-economic performance of dual-pressure evaporation ORC system also should be further quantitatively analyzed. In addition, for the dual-pressure evaporation ORC system, the selection of cycle parameters to obtain the optimal thermo-economic performance is an important issue in the system design whereas it is also unclear to date. Answering these issues is beneficial for the academic integrity and actual application of dual-pressure evaporation ORC system.

This study analyzed the thermo-economic performance of dual-pressure evaporation ORC system. The typical pure working fluid, R245fa, was used. R245fa has an attractive thermodynamic and thermo-economic performance in ORC systems (Imran *et al.*, 2016; and Wang *et al.*, 2011). The heat source is 100–200°C, and its outlet temperature has no specific limits (Li *et al.*, 2019). The heat exchangers are shell-and-tube type which are widely used in the ORC systems due to its good reliability, low cost and easy to maintain, and especially in the large ORC system. The working fluid flows in the tubes to better avoid the leaking. In this study, the pressures and evaporator outlet temperatures in two evaporation stages were optimized to achieve the lowest specific investment cost (SIC). The effects of heat source temperature, mass flow rate of heat source fluid, and PPTDs in the cycle heat transfer processes on the system thermo-economic performance were quantitatively analyzed. Finally, the thermo-economic performance of single-pressure and dual-pressure evaporation ORC systems was compared to evaluate the application potential of dual-pressure evaporation cycle.

2. ANALYSIS MODEL

The diagrams of dual-pressure evaporation ORC system are shown in Fig. 1. In this study, the heat source fluid is the hot water, and the heat sink is the cooling water. The ORC system consists of the shell-and-tube heat exchangers, axial-flow turbines and centrifugal feed pumps. The detailed flow paths of dual-pressure evaporation ORC can be referred to Li *et al.* (2018). The boundary conditions of dual-pressure evaporation ORC model can also be referred to Li *et al.* (2018). The system is assumed as in a steady state, and the pressure drop and heat loss in the heat exchangers and pipes are neglected. The evaporation pressures of two stages and evaporator outlet temperature in the high-pressure stage were optimized. The evaporator outlet temperature in the low-pressure stage was set as the lower limit to avoid the expansion process passing through the two-phase region (Li *et al.*, 2017b). The selectable ranges of high-stage evaporation pressure (p_{e_HP}), low-stage evaporation pressure (p_{e_LP}) and evaporator outlet temperature in the high-pressure stage (T_5) are $p_{cond} + 100$ kPa to $0.9p_c - 100$ kPa, $p_{e_LP} + 100$ kPa to $0.9p_c$, and the lower limit to $T_{HS,in} - \Delta T_{HAP,pp}$, respectively. The detailed reasons of these selectable ranges can be referred to Li *et al.* (2018).

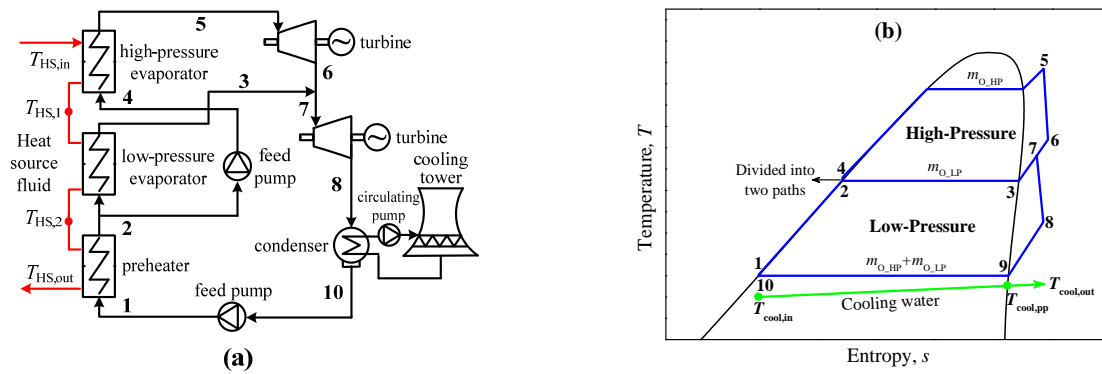


Figure 1: Diagrams of dual-pressure evaporation ORC system

The material of heat exchangers is the stainless steel, and the internal and external diameters of tube are 20 mm and 24 mm, respectively. The velocities of working fluid at the condenser and preheater inlets are 8 m/s and 1 m/s, respectively. The mass fluxes of working fluid are the same in the preheater and evaporators. The velocities of heat source fluid and cooling water outside the tubes are 1 m/s.

For the heat exchanger, the overall heat transfer coefficient in each section is calculated as follows:

$$\frac{1}{U} = \frac{1}{\alpha_i} \frac{d_o}{d_i} + R_i \frac{d_o}{d_i} + R_o + \frac{\delta_{wall}}{\lambda_{wall}} \frac{d_o}{d_m} + \frac{1}{\alpha_o} \quad (1)$$

where α_i and α_o are convection heat transfer coefficients inside and outside the tubes, respectively; and the calculations of them in various heat transfer processes can be referred to Li *et al.* (2017a).

The calculations of thermodynamic performance, such as the system efficiency, working fluid mass flow rates, and net power output, can be referred to the study of Li *et al.* (2018). The purchased equipment cost (*PEC*) of each component in the system is calculated as:

$$\log_{10} PEC^0 = K_1 + K_2 \log_{10} Y + K_3 [\log_{10} Y]^2 \quad (2)$$

where PEC^0 is the basic cost, \$; K_1 , K_2 , and K_3 are constants; Y is the heat transfer area for the heat exchanger, m^2 ; and is the power for the turbine and feed pump, kW.

The *PEC* of heat exchanger should further consider the effects of material and operating pressure:

$$PEC = PEC^0 F_{BM} = PEC^0 (B_1 + B_2 F_M F_P) \quad (3)$$

where B_1 and B_2 are constants, F_M and F_P are the material and pressure factors, respectively.

The *PEC* of each component should be further amended due to the effect of inflation:

$$PEC_{2017} = PEC_{2001} (CEPCI_{2017} / CEPCI_{2001}) \quad (4)$$

where $CEPCI_{2017}$ is 567.5 and $CEPCI_{2001}$ is 397.

The specific investment cost (*SIC*) of ORC system is defined as (Quoilin *et al.*, 2011):

$$SIC = PEC_{system} / W_{net} = 6.32 \sum_{i=1}^n PEC_i / W_{net} = 6.32 PEC_{total} / W_{net} \quad (5)$$

where PEC_{system} and W_{net} are the total investment cost and net power output of ORC system.

The optimization objective is to obtain the lowest *SIC* for the dual-pressure evaporation ORC system at various operating conditions. The thermophysical properties of fluids are from REFPROP 9.1 (Lemmon *et al.*, 2013). The optimization methods and details are similar to those in Li *et al.* (2018).

3. RESULTS AND DISCUSSION

3.1 Optimized evaporation pressures and evaporator outlet temperatures

In the dual-pressure evaporation ORC system, with the increase of $T_{HS,in}$, the qualitative variations of optimized evaporation pressures and evaporator outlet temperatures are similar for various mass flow rates of heat source fluid, cooling water temperature rises, and combinations of PPTDs (i.e., $\Delta T_{HAP,pp} + \Delta T_{HRP,pp}$). Fig. 2 shows the optimized evaporation pressures and evaporator outlet temperatures at various heat source inlet temperatures. As the $T_{HS,in}$ increases, the optimized low-stage evaporation pressure ($p_{e_LP,opt}$) increases with a high increment, and the optimized high-stage evaporation pressure ($p_{e_HP,opt}$) increases and the increment first increases and then decreases. For the $p_{e_HP,opt}$, the decrease of increment is attributed to the limit of its upper limit, and the $p_{e_HP,opt}$ reaches at $0.9p_c$ when the $T_{HS,in}$ is 200°C which means it cannot further increase.

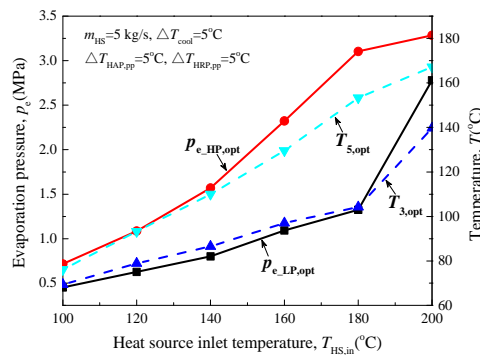


Figure 2: Optimized evaporation pressures and evaporator outlet temperatures at various heat source inlet temperatures

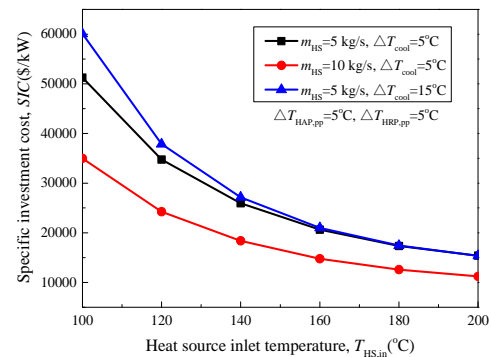


Figure 3: The SICs of dual-pressure evaporation ORC system at various mass flow rates of heat source fluid and cooling water temperature rises

As shown in Fig. 2, with the increase of $T_{HS,in}$, the variations of optimized low-pressure and high-pressure evaporator outlet temperatures are similar to those of $p_{e_LP,opt}$ and $p_{e_HP,opt}$, respectively. The optimized low-pressure evaporator outlet temperature ($T_{3,opt}$) is the lower limit corresponding to the $p_{e_LP,opt}$. The optimized high-pressure evaporator outlet temperature ($T_{5,opt}$) is higher than its lower limit when the $T_{HS,in}$ is $180\text{--}200^\circ\text{C}$, which means that a suitable superheat degree in the high-pressure evaporator is beneficial to obtain the lowest SIC. When the $T_{HS,in}$ is lower than 180°C , the minimum superheat degree in the high-pressure evaporator is more beneficial to obtain the lowest SIC.

3.2 SICs of dual-pressure evaporation ORC system

Fig. 3 shows the SICs of dual-pressure evaporation ORC system at various mass flow rates of heat source fluid and cooling water temperature rises. The SIC of dual-pressure evaporation ORC system decreases as the $T_{HS,in}$ increases, and the decrement also decreases. When the mass flow rate of heat source fluid is 5 kg/s and the cooling water temperature rise is 5°C , the SIC decreases from $51244\text{ } \$/\text{kW}$ to $15399\text{ } \$/\text{kW}$ as the $T_{HS,in}$ increases from 100°C to 200°C . As the mass flow rate of heat source fluid increases, the SIC of dual-pressure evaporation ORC system will significantly decrease. The main reason is that the increment of total investment cost increases with a low increment as the mass flow rate of heat source fluid increases; while, the net power output increases almost linearly. When the mass flow rate of heat source fluid increases from 5 kg/s to 10 kg/s , the SIC will decrease by $27.2\text{--}31.7\%$, and the decrement increases as the $T_{HS,in}$ decreases. With the increase of cooling water temperature rise, the SIC of dual-pressure evaporation ORC system will increase when the

$T_{HS,in}$ is low, whereas the increment decreases as the $T_{HS,in}$ increases. The SIC at the cooling water temperature rise of 15°C is even 0.3% lower than that at the cooling water temperature rise of 5°C when the $T_{HS,in}$ is 200°C . While, the SIC increases by 0.4%–17.2% when the cooling water temperature rise increases from 5°C to 15°C for the $T_{HS,in}$ of 100 – 180°C .

Fig. 4 shows the SIC s of dual-pressure evaporation ORC system at various combinations of PPTDs. Increasing the $\Delta T_{HAP,pp}$ and $\Delta T_{HRP,pp}$ is beneficial to reduce the SIC when the $T_{HS,in}$ is higher than approximately 170°C and 120°C , respectively. Thus, increasing the PPTDs in the cycle heat transfer processes is beneficial to reduce the SIC when the $T_{HS,in}$ is high; while, it is adverse when the $T_{HS,in}$ is low. In summary, in the dual-pressure evaporation ORC system using R245fa, the lowest SIC is obtained when the $\Delta T_{HAP,pp}$ and $\Delta T_{HRP,pp}$ are 5°C for the $T_{HS,in}$ below approximately 140°C . For the $T_{HS,in}$ above approximately 140°C , the lowest SIC is obtained at the $\Delta T_{HAP,pp}$ and $\Delta T_{HRP,pp}$ of 10°C .

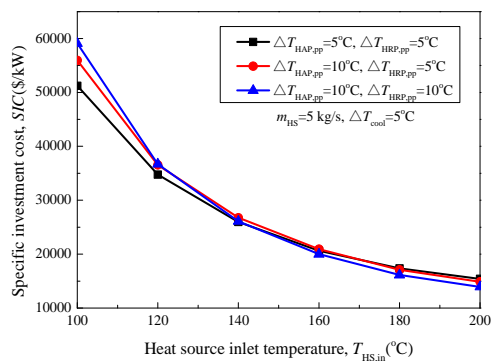


Figure 4: The SIC s of dual-pressure evaporation ORC system at various combinations of PPTDs

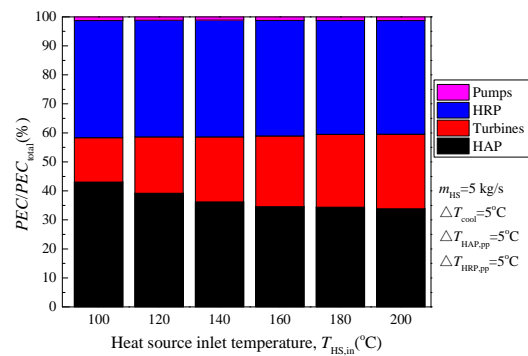


Figure 5: Ratios of the PEC for the components in the dual-pressure evaporation ORC system

3.3 Ratios of the PEC for the components

Fig. 5 shows the ratios of the PEC for the components in the dual-pressure evaporation ORC system. With the increase of $T_{HS,in}$, the ratio of the PEC of the heat absorbers (including the preheater, low-pressure and high-pressure evaporators) to the total PEC of components, PEC_{HAP}/PEC_{total} , decreases with a low decrement. The ratio of the PEC of turbines to the total PEC of components, PEC_T/PEC_{total} , increases with a low increment as the $T_{HS,in}$ increases. The ratio of the PEC of the condenser to the total PEC of components, PEC_{HRP}/PEC_{total} , nearly remains constant as the $T_{HS,in}$ increases. The ratio of the PEC of feed pumps to the total PEC of components, PEC_P/PEC_{total} , first decreases and then increases as the $T_{HS,in}$ increases. For the $T_{HS,in}$ of 100 – 200°C , the PEC_{HAP}/PEC_{total} , PEC_T/PEC_{total} , PEC_{HRP}/PEC_{total} , and PEC_P/PEC_{total} are 33.8%–43.1%, 15.3%–25.7%, 39.2%–40.4%, and 1.1%–1.3%, respectively. The PEC_{HRP}/PEC_{total} is the largest compared with other components when the $T_{HS,in}$ is higher than approximately 120°C , whereas it is lower than PEC_{HAP}/PEC_{total} when the $T_{HS,in}$ is 100°C . The PEC_P/PEC_{total} is the lowest.

For various cooling water temperature rises and combinations of PPTDs, with the increase of $T_{HS,in}$, the variations of the ratios of components are similar as shown in Fig. 5. As the mass flow rate of heat source fluid increases, the PEC_{HRP}/PEC_{total} increases, whereas the PEC_{HAP}/PEC_{total} and PEC_P/PEC_{total} decrease, and the PEC_T/PEC_{total} increases when the $T_{HS,in}$ is low whereas it decreases when the $T_{HS,in}$ is high. With the increase of cooling water temperature rise, the PEC_{HAP}/PEC_{total} and PEC_P/PEC_{total} increase, whereas the PEC_{HRP}/PEC_{total} decreases, and the

PEC_T/PEC_{total} decreases when the $T_{HS,in}$ is low whereas it increases when the $T_{HS,in}$ is high. The PEC_{HAP} will decrease as the $\Delta T_{HAP,pp}$ increases, and the PEC_{HRP} will decrease as the $\Delta T_{HRP,pp}$ increases. When the mass flow rate of heat source fluid is 5 kg/s and the cooling water temperature rise is 5°C, the PEC_{HAP}/PEC_{total} is the largest when the $\Delta T_{HAP,pp}$ and $\Delta T_{HRP,pp}$ are 10°C, whereas the PEC_{HRP}/PEC_{total} is the largest when the $\Delta T_{HAP,pp}$ is 10°C and $\Delta T_{HRP,pp}$ is 5°C, compared to other components. The variations of PEC_T and PEC_p are closely associated with the powers output by turbines and consumed by feed pumps, respectively. On the whole, the PEC_{HAP} and PEC_{HRP} are the two largest terms in the system at various operating conditions.

3.4 Comparisons of single-pressure and dual-pressure evaporation cycles

The conventional single-pressure evaporation cycle was selected as a comparison object to evaluate the application potential of dual-pressure evaporation cycle in the view of the thermo-economic performance. For the single-pressure evaporation cycle, the variations in SIC are similar as those of dual-pressure evaporation cycle with increasing the heat source inlet temperature, mass flow rate of heat source fluid, cooling water temperature rise, and PPTDs, as introduced in subsection 3.2. The electricity generation cost (EGC) was used to compare the thermo-economic performance of single-pressure and dual-pressure evaporation cycles more directly. The EGC is defined as:

$$EGC = (PEC_{system} \cdot CRF + AOC) / (W_{net} \tau_{OH}) \quad (6)$$

where $CRF = i(1+i)^n / [(1+i)^n - 1]$, i is the interest rate and selected as 5%, n is the system economic life and selected as 20 years; AOC is the annual operation and maintenance cost, and selected as $0.02PEC_{total}$; τ_{OH} is the annual operating hours and selected as 7200 h.

Fig. 6 shows the comparisons of the EGC between single-pressure and dual-pressure evaporation ORC systems. With increasing the mass flow rate of heat source fluid, cooling water temperature rise, and PPTDs, the variations of the EGC are similar as those of the SIC for the single-pressure and dual-pressure evaporation ORC systems. As shown in Fig.6, when the mass flow rate of heat source fluid is 5 kg/s, the $EGCs$ of the single-pressure and dual-pressure evaporation ORC systems are 0.160–0.545 $\$/kW \cdot h^{-1}$ and 0.178–0.594 $\$/kW \cdot h^{-1}$, respectively. When the mass flow rate of heat source fluid is 10 kg/s, the $EGCs$ of the single-pressure and dual-pressure evaporation ORC systems decrease to 0.119–0.381 $\$/kW \cdot h^{-1}$ and 0.130–0.405 $\$/kW \cdot h^{-1}$, respectively. Compared with the single-pressure evaporation ORC system, the EGC of dual-pressure evaporation ORC system increases by 8.0%–11.8% and 5.7%–9.6% when the mass flow rates of heat source fluid are 5 kg/s and 10 kg/s, respectively. The EGC of dual-pressure evaporation ORC system is higher which indicates its thermo-economic performance is worse. As the $T_{HS,in}$ increases, the increment of the EGC first decreases for the $T_{HS,in}$ below approximately 140°C and then increases for the $T_{HS,in}$ of 160–180°C, and finally decreases again. With the increases of cooling water temperature rise and $\Delta T_{HRP,pp}$, the increment in the EGC of dual-pressure evaporation cycle increases. While, the increment in the EGC of dual-pressure evaporation cycle decreases with the increase of $\Delta T_{HAP,pp}$. On the whole, the EGC of dual-pressure evaporation cycle increases by 5.7%–14.2% compared with that of single-pressure evaporation cycle within the whole studied operating conditions.

Fig. 7 shows the comparisons for the $PECs$ of the components between single-pressure and dual-pressure evaporation ORC systems. For other operating conditions, the compared results are similar as shown in Fig. 7. At the optimized operating conditions, the net power output of dual-pressure evaporation ORC system is 4.6%–27.2% larger than that of single-pressure evaporation ORC system, and the increment decreases as the $T_{HS,in}$ increases. Compared to the single-pressure evaporation ORC system, the summation of PEC_T , PEC_{HRP} , and PEC_p in the dual-pressure evaporation ORC system increases by 3.0%–15.7%, which is lower than the increment of net power output. The increment of

their summation also decreases as the $T_{HS,in}$ increases. While, the PEC_{HAP} increases by 51.1%–86.3% compared with that of single-pressure evaporation ORC system, which is significantly higher than the increment of net power output. Moreover, the PEC_{HAP}/PEC_{total} is 30.9%–38.5% for the dual-pressure evaporation ORC system. Hence, the higher SIC and EGC of dual-pressure evaporation cycle are mainly ascribed to the remarkable increase in the PEC_{HAP} .

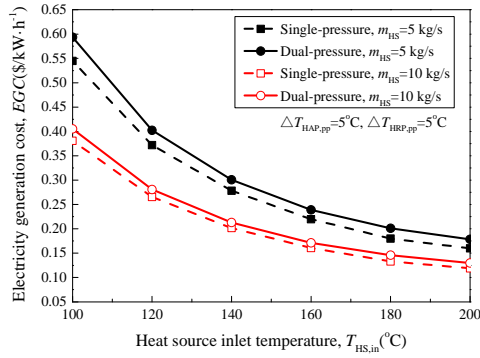


Figure 6: Comparisons of the EGC between single-pressure and dual-pressure evaporation ORC systems

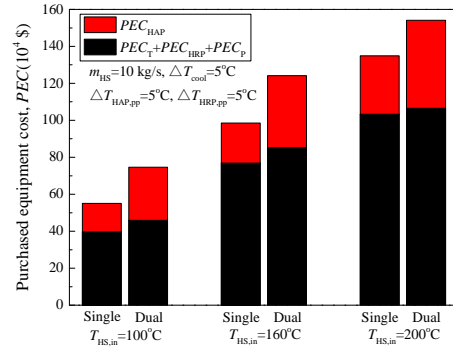


Figure 7: Comparisons for the $PECs$ of the components between single-pressure and dual-pressure evaporation ORC systems

For the dual-pressure evaporation ORC system, the remarkable increase of PEC_{HAP} is mainly caused by the decrease of heat transfer temperature difference between the heat source and working fluids, as well as the increase of heat absorption capacity; and these two factors significantly increase the total heat transfer area of heat exchangers. In summary, the dual-pressure evaporation cycle can significantly increase the heat-power conversion efficiency by reducing the heat transfer temperature difference between the heat source and working fluids. While, the SIC and EGC of dual-pressure evaporation cycle will be higher due to the remarkable increase in the PEC_{HAP} , and thus its thermo-economic performance is a little worse compared with the conventional single-pressure evaporation cycle. To help dual-pressure evaporation cycle obtain the better thermo-economic performance, reducing the PEC_{HAP} is an effective approach. Since reducing the $\Delta T_{HAP,pp}$ may increase the SIC ; thus, a suitable heat transfer enhancement method is more urgently needed.

4. CONCLUSIONS

The main conclusions are summarized as follows:

- The SIC of dual-pressure evaporation ORC system decreases as the $T_{HS,in}$ increases, and the decrement also decreases. Increasing the mass flow rate of heat source fluid will substantially reduce the SIC . The SIC of dual-pressure evaporation ORC system decreases by 27.2%–31.7% when the mass flow rate of heat source fluid increases from 5 kg/s to 10 kg/s.
- Increasing the PPTDs in the cycle heat transfer processes is beneficial to reduce the SIC at a high $T_{HS,in}$; while, it is adverse at a low $T_{HS,in}$.
- The PEC_{HAP} and PEC_{HRP} are the two largest terms in the system, and their ratios to the PEC_{total} are 30.9%–49.5% and 32.9%–43.7%, respectively.
- The EGC of dual-pressure evaporation ORC system is 5.7%–14.2% higher than that of single-pressure evaporation ORC system, and the worse thermo-economic performance of dual-pressure evaporation cycle is mainly ascribed to the remarkable increase in the PEC_{HAP} .

NOMENCLATURE

m mass flow rate (kg/s)

p	pressure	(MPa)
T	temperature	(°C)
W	power	(kW)

Subscript

1-10	state points in Fig.1
c	critical state
e	evaporation
HP	high-pressure stage
LP	low-pressure stage
opt	optimal
pp	pinch point

REFERENCES

- Imran, M., Haglind, F., Asim, M., *et al.*, 2018, Recent research trends in organic Rankine cycle technology: A bibliometric approach, *Renew. Sust. Energy Rev.*, vol. 81: p. 552-562.
- Imran, M., Usman, M., Park, B.S., *et al.*, 2016, Comparative assessment of Organic Rankine Cycle integration for low temperature geothermal heat source applications, *Energy*, vol. 102: p. 473-490.
- Lecompte, S., Huisseune, H., van den Broek M., *et al.*, 2015, Review of organic Rankine cycle (ORC) architectures for waste heat recovery, *Renew. Sust. Energy Rev.*, vol. 47: p. 448-461.
- Lemmon, E.W., Huber, M.L., McLinden, M.O., 2013, NIST reference fluid thermodynamic and transport properties–REFPROP, version 9.1, *National Institute of Standards and Technology, Standard Reference Data Program*, Gaithersburg.
- Li, J., Ge, Z., Duan, Y.Y., *et al.*, 2018, Parametric optimization and thermodynamic performance comparison of single-pressure and dual-pressure evaporation organic Rankine cycles, *Appl. Energy*, vol. 217: p. 409-421.
- Li, J., Ge, Z., Duan, Y.Y., *et al.*, 2019, Effects of heat source temperature and mixture composition on the combined superiority of dual-pressure evaporation organic Rankine cycle and zeotropic mixtures, *Energy*, vol. 174: p. 436-449.
- Li, J., Liu, Q., Duan, Y.Y., *et al.*, 2017a, Performance analysis of organic Rankine cycles using R600/R601a mixtures with liquid-separated condensation, *Appl. Energy*, vol. 190: p. 376-389.
- Li, J., Liu, Q., Ge, Z., *et al.*, 2017b, Thermodynamic performance analyses and optimization of subcritical and transcritical organic Rankine cycles using R1234ze(E) for 100–200°C heat sources, *Energy Convers. Manage.*, vol. 149: p. 140-154.
- Quoilin, S., Declaye, S., Tchanche, B.F., *et al.*, 2011, Thermo-economic optimization of waste heat recovery Organic Rankine Cycles, *Appl. Therm. Eng.*, vol. 31, no. 14-15: p. 2885-2893.
- Sadeghi, M., Nemati, A., Ghavimi, A., *et al.*, 2016, Thermodynamic analysis and multi-objective optimization of various ORC (organic Rankine cycle) configurations using zeotropic mixtures, *Energy*, vol. 109: p. 791-802.
- Shokati, N., Ranjbar, F., Yari, M., 2015, Exergoeconomic analysis and optimization of basic, dual-pressure and dual-fluid ORCs and Kalina geothermal power plants: A comparative study, *Renew. Energy*, vol. 83: p. 527-542.
- Velez, F., Segovia, J.J., Martin, M.C., *et al.*, 2012, A technical, economical and market review of organic Rankine cycles for the conversion of low-grade heat for power generation, *Renew. Sust. Energy Rev.*, vol. 16, no. 6: p. 4175-4189.
- Wang, E.H., Zhang, H.G., Fan, B.Y., *et al.*, 2011, Study of working fluid selection of organic Rankine cycle (ORC) for engine waste heat recovery, *Energy*, vol. 36, no. 5: p. 3406-3418.
- Ziviani, D., Beyene, A., Venturini, M., 2014, Advances and challenges in ORC systems modeling for low grade thermal energy recovery, *Appl. Energy*, vol. 121: p. 79-95.

ACKNOWLEDGEMENT

Financial supports from the National Natural Science Foundation of China (Grant Nos. 51736005 and 51621062) are gratefully acknowledged.